

# A Taguchi method-based optimization algorithm for the analysis of the wind driven-self-excited induction generator

Rachid Boukenoui<sup>1</sup>, Rafik Bradai<sup>2</sup>, Aissa Kheldoun<sup>3</sup>

<sup>1</sup>Electrical Systems and Remote-Control Laboratory (LabSET), Renewable Energy Department, Faculty of Technology, Blida 1 University, Blida, Algeria

<sup>2</sup>LATSI Laboratory, Automation and Electrical Engineering Department, Faculty of Technology, Blida 1 University, Blida, Algeria

<sup>3</sup>Laboratory of Signals and Systems, IGEE, University M'hamed Bougara, Boumerdes, Algeria

## Article Info

### Article history:

Received Jun 1, 2023

Revised Nov 28, 2023

Accepted Dec 7, 2023

### Keywords:

Induction generator

Optimization

Self-excitation

Taguchi's algorithm

Wind turbine

## ABSTRACT

This paper investigates the use of a new global optimization algorithm that is based on Taguchi method to determine the performance parameters of self-excited induction generator being driven by variable speed wind. This analysis is based on solving equations obtained from the per-phase equivalent circuit of the induction generator. The equations have two unknowns namely the frequency and the magnetizing reactance. Both unknown are strongly dependent on the wind turbine speed, the capacity of the excitation, the load being connected at the terminals of the stator and eventually the per-phase equivalent circuit parameters. The resulting equations are nonlinear and subsequently to solve them one can employ either gradient-based algorithms or heuristic algorithms. This paper uses a new heuristic algorithm based on the Taguchi method which, in addition to its global search capability, offers superior characteristics in terms of accuracy and ease of implementation. A comparison with recently published optimization methods is carried out to show its performances in terms of accuracy and ease of implementation. The MATLAB software will be used to perform this analysis on a machine of 0.75 kW while some will be validated experimentally to confirm the aforementioned benefits.

*This is an open access article under the [CC BY-SA](https://creativecommons.org/licenses/by-sa/4.0/) license.*



## Corresponding Author:

Rafik Bradai

LATSI Laboratory, Automation and Electrical Engineering Department, Faculty of Technology

Blida 1 University

BP270, Blida 09000, Algeria

Email: bradai\_rafik@univ-blida.dz or r.bradai@gmail.com

## NOMENCLATURE

$L_M(q^m)$  : Orthogonal array (OA)

$LD$  : Level difference

$\eta$  : Thes/N or Signal-to-Noise ratio

$J_k$  : The  $k$ -th fitness or cost function value

$m$  : Maximum number of factors or variables

$M$  : Minimum number of experiments

$p_j$  : The  $j$ -th factor

$T$  : Total number of iterations

$t$  : Iteration number

$C$  : Excitation capacitance per-phase,  $\mu\text{f}$

$F$  : Per unit frequency

$R_r$  : Rotor resistance referred to stator side

$R_M$  : Iron loss resistance

$X_r$  : Rotor reactance referred to stator side

$X_s$  : Stator reactance

$X_C$  : Capacitive reactance due to  $C$  at rated frequency

$X_0$  : Unsaturated value of magnetizing reactance

$X_M$  : Magnetizing reactance at rated frequency

$v$  : Per unit speed

$V_g$  : Air gap voltage per-phase at rated frequency

$V_l$  : Terminal voltage per-phase

$Y$  : Total admittance

$I_r$	: Rotor current referred to stator	$Y_A$	: Air-gap admittance
$I_s$	: Stator current	$Y_r$	: Rotor admittance
$I_L$	: Load current	$Y_s$	: Stator admittance
$N$	: Rated speed, rpm	$Y_L$	: Load admittance
$R_s$	: Stator resistance	$Y_C$	: Capacitive admittance
$R_L$	: Load resistance	$Y_M$	: Magnetizing admittance

## 1. INTRODUCTION

The constantly increase of electric energy use and cost rising of traditional energy sources required for the operation of power plants, together with the alarming concerns regarding the harmful effects of these plants on the environment have led to intensive research to promote the integration of renewable energies, which substantially reduce the CO<sub>2</sub> emissions. On the ground, several countries around the world have already set a deadline or a percentage of renewable energy sharing with respect to the total power demand. This can be accomplished by incorporating more renewable energy sources through the so-called smart grid and replacing in remote sites fossil fuel generators by photovoltaic, wind turbines or micro-hydro power plants [1]. The use of a renewable source at isolated sites is a cost-effective solution compared to the extension of the network or the use of diesel generators [2].

The use of squirrel cage asynchronous machine in isolated areas to convert wind energy into electrical energy has many advantages such as high reliability, low cost, maintenance free, self-protection against faults and overloads, and robust construction and ease of operation [3], [4]. Concerning the control of self-excited induction generator (SEIG), a high-performance maximum power point tracking (MPPT) strategy in the presence of iron losses and nonlinear magnetic characteristic is developed in [5], this strategy aims to: i) reduce the rotor and stator currents by taking control of the rotor flux and ii) capture the maximum wind power for insuring a high MPPT accuracy. Another control strategy for voltage regulation of a SEIG wind turbine based on the association of fuzzy logic and a sliding mode controller is presented in [6]. The dynamic operation of SEIG in steady state and no-load operation is investigated in [7] by using a neuro-fuzzy controller (NFL) for regulating the generated voltage and frequency. Compared to PI controller, the NFL shows more accuracy and fast response. A modified near field communication (NFC) is applied in [8] to promote the voltage and frequency regulation of the SEIG. However, in addition to increased computational burden of NFL, such strategy may lead to delayed response and ambiguous results. By comparing the asynchronous machine with its synchronous counterpart, the asynchronous machine receives its need in terms of reactive power from the network utility, being not available in isolated areas, a source of this energy is necessary for the machine to convert wind energy into electrical energy. Indeed, if a right capacitor battery is placed across the squirrel cage induction machine and the latter is driven at the desired speed, the residual flux in the machine will induce a low voltage within the stator, which is looped on the capacitor. The latter generates a reactive current and increases the rotor flux which in turn will boost the reactive current and the stator voltage. This interaction process between the capacitor connected on the stator and the magnetic circuit is named the phenomenon of self-excitation [3], [9], [10]. Eventually the stator voltage settles down to a point defined by the intersection of the magnetization curve and the capacitor charging line. The amplitude and frequency of the voltage obtained at the terminals of the stator strongly depend on the rotor speed, the impedance of the load, the excitation capacity, the parameters of the equivalent circuit and the magnetization characteristic. This makes the determination of the voltage parameters as well as the machine performance parameters a difficult task to achieve.

Computing performance parameters of the self-excited squirrel cage asynchronous machine depends on employing the machine's per-phase corresponding circuit. It means, either loop analysis techniques [11]–[14] or nodal analysis ones [3], [15]–[17] will be employed for evaluating these parameters. The last-mentioned techniques derivate the admittance (or impedance) equation to be segregated into a real and imaginary parts. The next move employs the Newton-Raphson algorithm for solving these equations and achieving the suitable values of the frequency (F) and the magnetizing reactance (XM). Authors in [18]–[22], alleviate the computation process by employing equations derived from the nodal analysis. To this end, an iterative algorithm is applied to solve just the real part of the admittance equation. This allows obtaining the value of F that should be used in the imaginary equation for deducing the XM value. However, the two techniques mentioned previously have the following disadvantages: i) the need for segregation of the impedance equation into real and imaginary parts and ii) the mandatory use of an iterative algorithm whose performance depends on a suitable selection of initial-parameters. To overcome this, heuristic algorithms such as genetic algorithms (GAs) are used [23], [24] which take the impedance equation as a black box. The solution of the equation impedance being equating to zero is reformulated as an unconstrained optimization problem. Mathematically, the convergence to best solution of the equation cannot be ensured and therefore the optimization's accuracy may not be satisfactory. For this, GAs is usually associated with a gradient-based optimization algorithm; in the

first stage GAs are performed to find an approximate solution of the problem, which will be used in the second stage by a gradient-based algorithm to reach the optimal solution.

Another artificial intelligence (AI) technique, fuzzy logic (FL), has been used for the steady state analysis of single-phase SEIG [25]. However, besides the computational burden required for the implementation of FL inference system, the use of this technique for the steady state analysis is yet to be justified, when compared with global search algorithms. Furthermore, proper choice of the initial guess remains a requirement.

Pre-programmed optimization techniques have been gaining popularity recently; they can be found in the toolboxes of software devoted to engineering computations such as MATLAB. These techniques can be employed for minimizing the impedance (i.e., into imaginary and real parts) without any passage by the segregation step. The function "Constr" provided by MATLAB was applied by Alolah and Alkanhal [18] for obtaining the optimal values of: admittance, F and XM. Those values are then applied for studying the SEIG performance. The second function "fsolve" provided by MATLAB was used by Haque [19], [20] to get the optimal value of impedance, meanwhile, analyzing the machine performance in different operating conditions (i.e., during constant stator voltage or current constraints). Singh *et al.* [26], [27] carried out the performance analysis through using the equivalent circuit of six-phase induction machine. It's important to mention that "fmincon" function was chosen to minimize the absolute value of the overall admittance. The goal was to find the best values of shunt and series capacitor, needed for the self-excitation of the six-phase SEIG. These built-in functions have demonstrated a high efficiency in optimizing admittance (or impedance) equations. This advantage leads to find the optimal values of XM and F, avoiding the tedious and time-consuming process of segregating the impedance or admittance equations. However, to implement these functions, it is mandatory to find a suitable initial guess, which needs a basic understanding of the problem in order to estimate it. A dynamic model that of wind driven SEIG is developed in [28] for analyzing the system performance during both transient and steady-state conditions. However, the analytical formulas used in this model are based on all the parameters of SEIG for the calculation of the rotor speed and excitation capacitance. Concerning the excitation capacitance, a detailed study of the iron losses influences on choosing the minimum excitation capacitance for SEIG with wind turbine is presented in [29]. The evaluation of eddy current losses is helpful during the design stage of the machine in order to obtain maximum efficiency. For this purpose, Dalabeeh *et al.* [30] model the effect settings on the eddy current losses in wind driven SEIG.

The afore-mentioned drawbacks of local optimizers, such as FL as well as built-in functions, can be overcome by applying the direct global optimization methods [31]. However, direct's convergence time directly depends on the range of the problem's search space. This is due to the fact that direct utilizes the concept of splitting the search space into other tiniest search spaces and assessing their midpoints. Potentially optimal rectangles are subsequently identified and studied during the following iteration. The wider is the search space, the more rectangle division is necessary and therefore longer time is essential for reaching the optimal solution. This dependence on the search space selection for global optimizers as well as the tedious task of finding the appropriate initial parameters for local search algorithms are circumvented by a Taguchi method-based optimization algorithm described in detail in the present work. The Taguchi algorithm uses the orthogonal arrays (OAs) which set the minimum number of experiments from which effects of multiple factors with different levels are to be investigated simultaneously to arrive at the optimum combination of levels. It is worth mentioning that, in addition to the global research capability of Taguchi algorithm, it offers superior characteristics when it comes to accuracy and ease of implementation, particularly, in the analysis of SEIG's steady state parameters. Therefore, a comparison with three recently published optimization methods such as: direct [31], fsolve [19], [20] and cuckoo search (CS) algorithm [32] is carried out to prove its performances. Moreover, the computed results are compared to the experimental one quoted from [18].

The remaining of the paper is organized as follows: i) Section 2, the problem of steady state analysis of the SEIG is formulated; ii) Section 3 undertakes the description of the Taguchi's method; iii) Section 4 presents the methodology of using Taguchi in the analysis of the SEIG performance characteristics; iv) Obtained results using Taguchi method and their discussions are presented in section 5; v) The comparison of Taguchi algorithm with other methods is provided in section 6; vi) Section 7 provides an experimental validation of some predicted results; and vii) Finally, a general conclusion is reported in the last section.

## 2. FORMULATION OF THE PROBLEM

Performance evaluation of the self-excited squirrel cage induction machine is essentially based on the determination of machine parameters such as power factor, active and reactive power output, efficiency, and stator voltage, under different operating conditions defined by external parameters, namely: the impedance of the load at the stator terminals, the excitation capacity value and the speed at which the rotor is spin. The first objective of such analysis is the determination of requirements on external parameters without which self-excitation cannot occur. These requirements can be determined through using the equivalent

circuit for each phase of the asynchronous machine depicted in Figure 1. As mentioned earlier, we can employ either nodal analysis or loop analysis. In the paper, the nodal analysis is used.

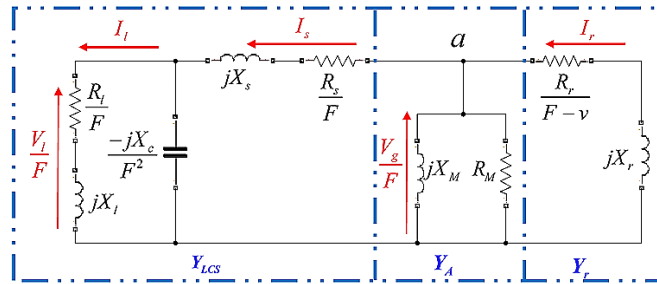


Figure 1. Per-phase equivalent circuit of SEIG

Upon the application of Kirchoff's current law to node  $a$  (i.e., shown in Figure 1), the necessary condition required by the self-excitation process is that the capacitor voltage is not equal zero, resulting in a null absolute value of the total admittance, as specified from (1) to (9) [31]. To solve these equations and find the values of  $F$  and  $X_M$ , as explained in the introduction, two main ways are possible. The first one is classic using a gradient-based algorithm while the other is based on optimization.

$$|\bar{Y}| = 0 \quad (1)$$

Where:

$$\bar{Y} = \bar{Y}_{LCS} + \bar{Y}_A + \bar{Y}_r \quad (2)$$

$$\bar{Y}_A = -j \cdot \frac{1}{X_M} + \frac{1}{R_M} \quad (3)$$

$$\bar{Y}_r = \frac{1}{\frac{R_r}{F-v} + jX_r} \quad (4)$$

$$\bar{Y}_C = j \cdot \frac{F^2}{X_C} \quad (5)$$

$$\bar{Y}_L = \frac{1}{\frac{R_L}{F} + jX_L} \quad (6)$$

$$\bar{Y}_s = \frac{1}{\frac{R_s}{F} + jX_s} \quad (7)$$

$$\bar{Y}_{LCS} = \frac{(\bar{Y}_L + \bar{Y}_C) \cdot \bar{Y}_s}{\bar{Y}_L + \bar{Y}_C + \bar{Y}_s} \quad (8)$$

$$|\bar{Y}| = \sqrt{(\text{Re}(\bar{Y}))^2 + (\text{Im}(\bar{Y}))^2} \quad (9)$$

### 3. STEADY STATE ANALYSIS USING OPTIMIZATION

The optimization is defined as the process of seeking the optimum point of continuous or discrete mathematical multivariable functions. A multivariable function may have one or more than one optimum point which is the maxima or the minima within a given interval. Local search algorithms are used to find the optimum solution of (1) when this latter has only one optimum point within a given interval. This type of algorithm would fail to find the global solution when the function has more than one solution within a given interval. In other words, the multivariable function has several optimum points; one of them is known as the global optimum point and the remaining are called the local optimum points. The type of algorithm that can

be employed for the above-mentioned situation is known as a global search algorithm. In the case of the SEIG analysis problem, the multivariable function is the admittance being equated to zero. In other words, the admittance absolute value is zero which represents its minimum point. Therefore, solution for  $X_M$  and  $F$  of (1) can be converted to seeking the optimum point ( $X_M, F$ ) leading to the minimum value of the admittance absolute value,

$$\text{Minimize } |\bar{Y}| \text{ subject to: } \begin{cases} 0 \leq F \leq v \text{ (input rotor speed)} \\ 0 \leq X_M \leq X_0 \text{ (unsaturated value)} \end{cases}$$

Using the optimization method allows preventing the disadvantages of the conventional approach. The integrated functions of MATLAB namely "fsolve", "fmincon", "constr" or of MathCAD "Find" and "Given" and others were used as optimizers. The drawback of applying built-in functions is the need to provide an initial solution. Some heuristic algorithms, such as: direct and GAs have been employed to minimize as (1) where the research space boundaries were derived from the constraints of the problem [24], [27]. However, the optimization accuracy is highly influenced by the search space selection, in other words, wide search space will result in a slow convergence and sometimes the result's accuracy is not sufficient. In the paper, the Taguchi method is used for minimizing the admittance equation, that is the (1). The optimization is implemented by preserving the equations of the admittance as obtained from nodal analysis. In other words, no longer need to separate the admittance equation into real and imaginary parts and to have the basic knowledge to providing a suitable initial solution. The optimal solution ( $X_M, F$ ) is obtained after the Taguchi method has converged to the minimum of the cost function, namely the admittance in (1). These are the key parameters for evaluating the performance of the SEIG. The induced voltage ( $V_g/F$ ) is determined using the magnetization curve which is approached by a 3rd order polynomial expression, which is approached by a 3rd order polynomial expression given as (10).

$$V_g/F = A_3.XM^3 + A_2.XM^2 + A_1.XM + A_0 \quad (10)$$

Where,  $A_3 = -0.418359$ ,  $A_2 = 1.8711$ ,  $A_1 = -2.92318$  and  $A_0 = 2.5954$ .

Other parameters characterizing the asynchronous generator such as voltage, current and power at different points of the same passive periodic excitation case (PPEC) are forwardly derived using the value  $V_g/F$ . For the sake of simplifying the computation, the air-gap voltage is taken as a reference phasor ( $\bar{V}_g = V_g \angle 0^\circ$ ). Therefore, stator current, output voltage and load current phasors are given by (11)-(13), respectively.

$$\bar{I}_s = \frac{\bar{V}_g}{F} \cdot (\bar{Y}_A + \bar{Y}_r) \quad (11)$$

$$\bar{V}_L = \bar{I}_s \cdot (\bar{Y}_L + \bar{Y}_C)^{-1} \cdot F \quad (12)$$

$$\bar{I}_L = \frac{\bar{V}_L}{F} \cdot \bar{Y}_L \quad (13)$$

Finally, the real power delivered to the load is given by (14).

$$P = 3 \cdot R_L \cdot |\bar{I}_L|^2 \quad (14)$$

## 4. TAGUCHI METHOD BASED ANALYSIS

### 4.1. Taguchi method

Modern industry is based on the design process and therefore their optimization is extremely important. The design of an industrial product and its quality depend on several factors, full number of experiments is usually conducted to compare factor levels with each other. A table of response is obtained by varying levels of each factor and realizing all relevant experiences. This process of conducting experiences is repeated as many as it takes to achieve the desired quality. This method of optimization by combining all experiments is called "full factorial experiment". The Taguchi method is distinguished as a method of "fractional factorial experiment", because it can effectively reduce the number of tests without affecting the optimal solution. It uses the concepts of orthogonal-arrays (OA) and signal-to-noise-ratios (S/N) [33].

Orthogonal arrays determine the number and the way how to conduct experiments for a given number of factors and levels. It combines experiences in such way that enough information is obtained about

effects of each level of each factor. Each parameter in the designation of AO, or  $L_M(q^m)$ , has a meaning;  $q$  is the levels number featuring each factor,  $m$  is the factors maximum number, and  $M$  is the minimum experiments number to obtain data characterizing the interactions between factors and the effects of their levels. The OA selection depends on the factors number and their levels. It is obtained by using available codes for the generation of OAs or directly from special libraries [33]. An OA example;  $L_9(3^4)$  is shown in Table 1, where  $m = 4$  (i.e., number of factors),  $q = 3$  (i.e., number of levels) and  $M = 9$  (i.e., minimum number of experiments).

By analyzing Table 1, we can notice that the time of occurrence of levels for each factor is the same. The same notice regarding the combination of each two factors. An important property of OA to be used later in this work is when for a problem with a given factors number, there is no appropriate OA. In this case, we can take an existing AO with a number of columns (factors) greater than the factors number of the problem; keep as many columns as the factors number of the problem then remove the remaining columns. The reduced table is an AO having a reduced number of factors. However, many OAs with greater number of columns are available in the library and selection of one becomes an optimization problem too.

Table 1. Orthogonal array  $L_9(3^4)$

$L_9(3^4)$		Problem factors				$L_9(3^4)$		Problem factors			
Experiments		p <sub>1</sub>	p <sub>2</sub>	p <sub>3</sub>	p <sub>4</sub>	Experiments		p <sub>1</sub>	p <sub>2</sub>	p <sub>3</sub>	p <sub>4</sub>
1		1	1	1	1	6		2	3	1	2
2		1	2	2	2	7		3	1	3	2
3		1	3	3	3	8		3	2	1	3
4		2	1	2	3	9		3	3	2	1
5		2	2	3	1						

Related to Taguchi's S/N, once experiments mentioned by the selected OA are conducted, the next step would be the analysis of data to identify the optimal levels for factors. This analysis begins by calculating the fitness function tendency for each factor through the use of S/N. Three different S/N are mostly employed in optimization [34], which are: smaller-the-better, nominal-the-best and larger-the-better. In accordance with the objective of optimization, one can select the appropriate ratio. In the paper, the goal is to minimize the admittance absolute value (which is theoretically zero), the smaller-the-better ratio appears to be more suitable and it is given as [35].

Using (15), the S/N ratio is computed for each experiment out of the nine experiments. One can figure out that the higher the S/N ratio the smaller the cost function's value will be. The obtained results allow constructing a response table by determining the average S/N ratios for each factor and each level. The optimal level for each factor can be then obtained and employed for the computation of the new levels and the corresponding minimum fitness function. This process is repeated until the admittance's minimum is reached. The optimization process is halt by verifying at each iteration a given termination criterion.

$$\eta = -10 \log_{10}(|\bar{Y}|) \quad (15)$$

#### 4.2. Minimization of admittance using Taguchi method

This subsection is devoted to the application of Taguchi method for solving the admittance equation and the evaluation of the SEIG performance parameters using the obtained optimal solution. The two main concepts of Taguchi optimization process developed in the previous section will be detailed in this section by developing each step alone:

- Step (a) which is the selection of OA and problem initialization. The application of Taguchi's optimization method begins as mentioned before by selecting the appropriate OA and setting the fitness or cost function (CF). Selection of OA must be done according to the number of factors or parameters which are of 2 ( $X_M$  and  $F$ ) in our case. By looking at the OA library, the OA  $L_9(3^4)$  is selected for our problem. As the number of parameters is only two, only the first two columns are kept, as shown in Table 1. In order to characterize the non-linear effect, three levels are needed for each factor. The cost function is the absolute value of the admittance as (9) while S/N ratio is calculated using (15).
- Step (b) which is computation of factor levels. To conduct the nine experiments specified by the OA cycle, levels being denoted by 1, 2 and 3 must be converted to their appropriate numerical values. To this, the middle level that is 2 is first computed and the remaining levels will be derived using the level difference's value being adopted. In the first iteration, level 2 of each parameter or factor is taken to be the middle of the search space [33]. The level difference is initialized using (16).

$$LD_j^1 = \frac{upper(j)-lower(j)}{numberoflevels+1} \tag{16}$$

Where: the subscript j denotes the parameter p<sub>j</sub>, the superscript 1 denotes the first iteration. In the nominator, upper (p<sub>j</sub>) and lower (p<sub>j</sub>) are the search space limits of factor p<sub>j</sub>. In the paper, the lower values of the two factors used in the application of Taguchi’s algorithm are respectively {0.01, 0.01} while the upper values are {45, 2}.

- Step (c) which is the S/N ratio computation and levels contribution. Table 2 shows conversion from levels to numerical values of factors. For each experiment J<sub>k</sub>, characterized by values of the two factors, XM and F in the orthogonal array, the fitness or cost function and the S/N ratio are evaluated. After that, the total contribution of each level and for each factor is computed using (17). Table 3 gives the results of the application of (17) which are the values of the contribution of each level for each factor during the first iteration.

$$\eta_{avg}(i, j) = \frac{q \cdot \sum_{k, OA(k,j)=i} \eta_k}{M} \tag{17}$$

Table 2. Level values, fitness values and S/N ratios of the first iteration

Experiments, J <sub>k</sub>	Level values		Y , Ω <sup>-1</sup>	S/N ratio (dB)
	X <sub>m</sub>	F		
1	18.055	0.955	0.3196	9.9085
2	18.055	1.050	1.0883	-0.7347
3	18.055	1.145	1.9684	-5.8821
4	20.050	0.955	0.3250	9.7614
5	20.050	1.050	1.0913	-0.7587
6	20.050	1.145	1.9704	-5.8911
7	22.045	0.955	0.3295	9.6427
8	22.045	1.050	1.0938	-0.7785
9	22.045	1.145	1.9721	-5.8985

Table 3. Response table of the first iteration

Average S/N ratio (dB)		Factors	
		X <sub>m</sub>	F
	Level 1	1.0972	9.7709
	Level 2	1.0372	-0.7573
	Level 3	0.9886	-5.8906

- Step (d) which is the identification of optimal level values. The largest value of the average S/N ratio which means the smallest value of the admittance’s absolute value corresponds actually to the optimal level for that factor. Once the optimal level value for each factor is obtained, the best minimum of the admittance for the current cycle is calculated. For example, from Table 3 we can easily identify the optimum levels for the first iteration which are: level 1 for the factor XM and level 1 too for factor F. The combination of these optimal levels is considered as the optimal solution candidate up to this iteration. This solution is used after that to conduct another experiment which may or not be among the OA’s nine experiments to calculate the current best fitness value. The current best fitness value will be used to check the termination criterion that is chosen to be J<sub>min</sub> (t) - J<sub>min</sub> (t-10) ≤ ε. Where t is the iteration number and ε is the error criterion chosen by the user according to the desired precision. The algorithm is terminated if either there is no more improvement in the optimum solution or the maximum number of iterations is exceeded.
- Step (e) which is updating the level values. In case the termination criterion is not satisfied or the maximum number of iterations is not exceeded, the level values must be updated for the next cycle. First the level 2 will take the optimal solution value of the current cycle and the remaining levels are updated with the same procedure of the initialisation with the level difference being modified according to (18).

$$LD_j^t = LD_j^{t-1} \cdot e^{-\left(\frac{t}{T}\right)^2} \tag{18}$$

Where T is the duration width of the Gaussian function and t is the current iteration. The next iteration starts by updating the orthogonal array by using the new level values to conduct the new experiments then repeat steps (b) then (c) followed by (d) and finally (e) till the termination criterion is satisfied. Figure 2 depicts the flowchart which summarizes the above-mentioned steps of Taguchi optimization algorithm to minimize the SEIG’s admittance absolute value.

For the sake of test, Figure 3 shows the fitness or the minimum found of the admittance during the whole iterative optimization process for the following external parameters: rotor speed  $v=1.1pu$ , excitation capacitance  $C = 25\mu F$  and a load impedance  $Z_L = 1\angle 0^\circ pu$ . The optimization process has been ended by the fact that there was no more improvement in finding the minimum value of the admittance. The number of iterations seems to be high however the number of function evaluation by iteration is only 9 which give a total of 900 evaluations. The optimized global minimum found is  $2.24 \cdot 10^{-16}$  corresponding to the optimal solution of  $(X_M, F) = (2.8339pu, 0.9498pu)$ .

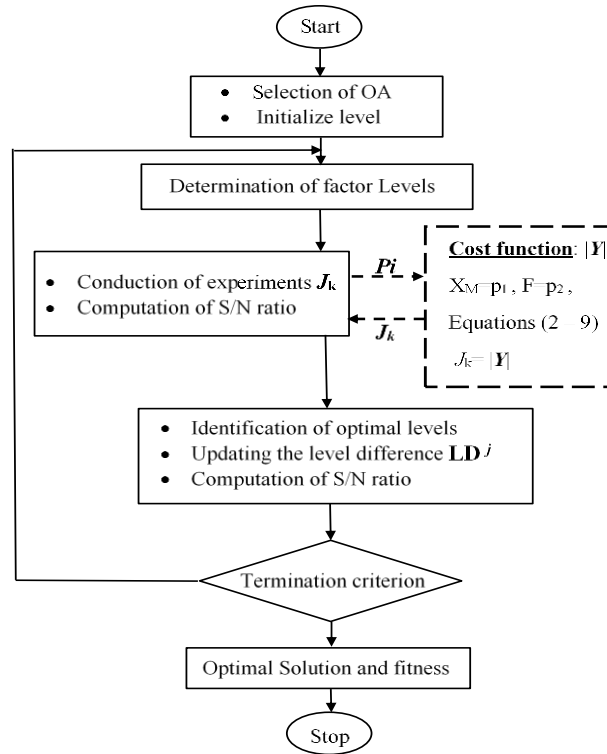


Figure 2. Flowchart of the Taguchi algorithm being used in the minimization of the absolute value of the admittance

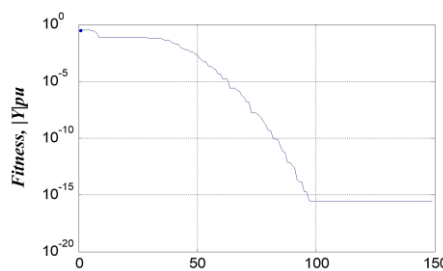


Figure 3. Minimum of the cost function found by Taguchi algorithm versus iteration

### 5. COMPUTATION RESULTS AND DISCUSSION

Performance parameters of SEIG are calculated by obtaining first the solution of (1); which are the values of  $X_M$  and  $F$ . Using these values as well as the saturation characteristic (shown in (10)) of the studied machine, the air-gap voltage ( $V_g$ ) is calculated. Finally, the output parameters which represent the performance characteristics of the generator namely: the stator current, the load current, the output voltage, and the output power are evaluated using (11)-(14). In the following two subsections, the optimization accuracy using Taguchi method in obtaining the solution for the SEIG analysis is assessed; the input parameters, which alter both the self-excitation process and output parameters of the SEIG are varied. That



is, the optimizer should provide the appropriate values of  $F$  and  $X_M$  (global optimum solution) to be used in the performance parameters evaluation. To this end, two loops are executed simultaneously in which the inner one involves the load impedance variation while the external loop is the rotor speed or the excitation capacitance loop. For each combination of the rotor speed, load impedance and excitation capacitance, the Taguchi algorithm shown in Figure 2 is run for solving (1) for  $X_M$  and  $F$  values. High accuracy computation of  $X_M$  and  $F$  is of great significance as their values are used in the evaluation of all performance parameters.

### 5.1. Minimization of admittance using Taguchi method

The first test concerns the rotor speed variation of the SEIG (i.e., the multiplication of the gearbox ratio and the wind turbine speed). The randomness of the wind speed directly affects the one of the turbines. The latter has direct influence on both the self-excitation process and the machine performance. The evaluation method of this effect is as follows: the excitation capacitance value is kept constant ( $C = 25\mu\text{F}$ ) while the rotor speed is changed within a specific range. It is worth mentioning that for each speed value, the load impedance to which the machine provides power varies from a minimum value to a value that renders the machine unloaded, the performance parameters variation is saved. Figure 4 and Figure 5 show respectively the  $X_M$  and  $F$  values obtained from minimizing the admittance's absolute value by the Taguchi method. Figure 6 clearly illustrates the optimization performance of the Taguchi algorithm and this regardless of the specified values of the rotor speed or the load impedance. One can notice from the same figure that the average value of the minimum obtained by Taguchi algorithm is about  $10^{-15}$ .

The results show that induction generator cannot operate if the unsaturated value is lower than magnetizing reactance provided by the optimizer. In other words, self-excitation process cannot take place. An example can be taken from Figure 4, the rotor speed  $v=0.9$  pu and the load impedance  $Z_L$  is less than 1.5 pu, the figure shows that  $X_M$  is greater than  $X_0$ , which leads to failure of self-excitation. Moreover, sometimes although  $X_M$  is less than the unsaturated value which means there is self-excitation for a given external parameters (i.e., capacitance, rotor speed and load impedance values), the generator's operating point is within the unstable region. The latter is identified by points in the curve of  $X_M$  which are situated within the curve's bended region. In Figure 7 the unstable region is illustrated by a positive slope while normal operation region has a negative slope (e.g. the voltage decreases as the supplied active power increases). It can be deduced also from Figure 7 that narrower normal operating region of the asynchronous generator results when  $X_M$  is closer to  $X_0$ .

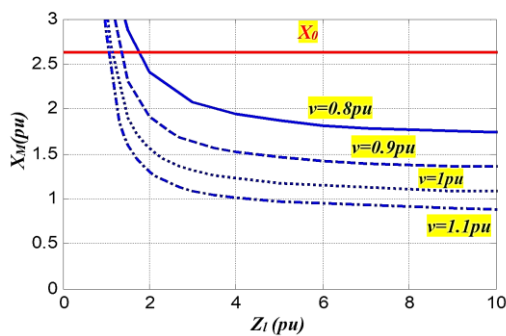


Figure 4. Magnetizing reactance ( $X_M$ ) versus load variation for different speeds and  $C=25\mu\text{F}$

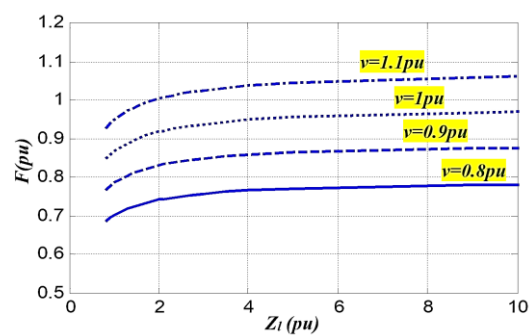


Figure 5. Frequency ( $F$ ) versus load variation and different speeds with  $C=25\mu\text{F}$

### 5.2. Variation of excitation capacitance and load impedance

The second important external parameter is the capacitance of the capacitor bank connected to the induction generator's stator terminals. The rotor speed is now set to 1.1 pu and the capacitance is varied from  $15\mu\text{F}$  to  $35\mu\text{F}$ . The  $X_M$  and  $F$  values resulted by the Taguchi's optimization algorithm are illustrated in both, Figure 8 and Figure 9, respectively. Figure 10 shows the optimization performance of Taguchi's algorithm which is the minimum admittance *w.r.t* load impedance. The average value of the accuracy is about  $10^{-15}$  which seems to be very satisfactory. Besides, it shows the ability of Taguchi's algorithm in achieving the global optimal solution even for large external parameters variations.

Upon comparison of results depicted in Figure 5 and Figure 9, it is worth noting that the output frequency has a great dependence on the prime mover speed, meanwhile, it is less sensitive to the excitation capacitance. Moreover, from the results depicted of Figure 11, one can notice that the capacitance increases

leads to enlarging the normal operating region and increasing the power delivering capability of the SEIG. However, the SEIG will always have a maximum power which is the point where the curve bends.

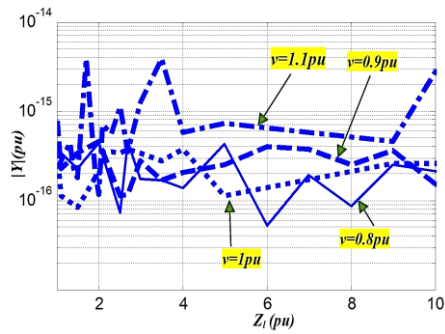


Figure 6. Minimum admittance found by Taguchi algorithm with  $C=25\mu F$

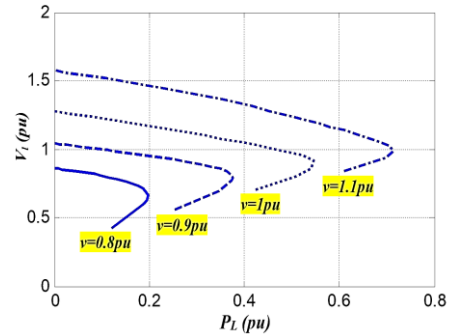


Figure 7. Output voltage versus real power variation for different speeds with  $C=25\mu F$

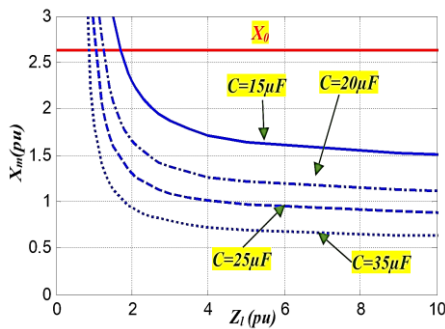


Figure 8. Magnetizing reactance ( $X_M$ ) versus load variation for different capacitance and  $v=1.1pu$

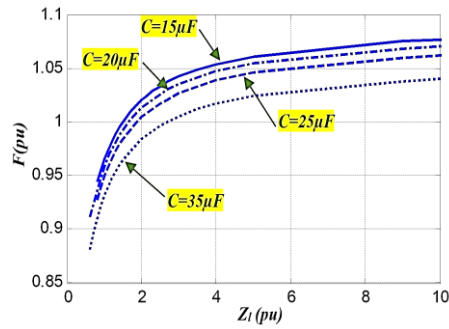


Figure 9. Frequency ( $F$ ) versus load variation for different capacitance and  $v=1.1pu$

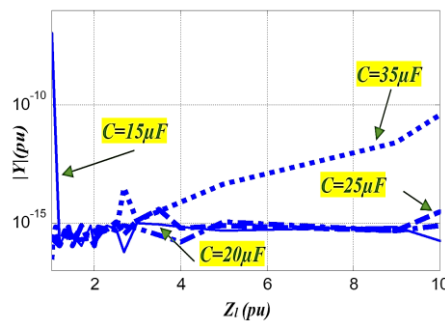


Figure 10. Minimum admittance found by Taguchi algorithm,  $v=1.1pu$

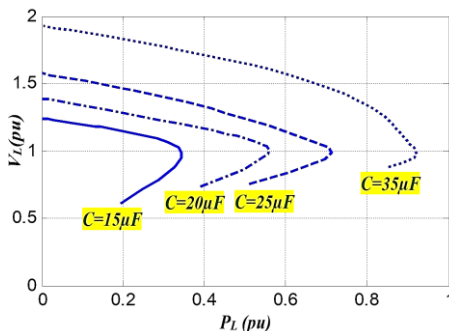


Figure 11. Output voltage versus real power variation for different capacitances and  $v=1.1pu$

### 6. ASSESSMENT OF TAGUCHI ALGORITHM

To show the performances of Taguchi algorithm in the analysis of SEIG's steady state parameters, it has been compared with recently applied algorithm for the same purpose. Table 4 depicts the comparison of Taguchi with direct, fsolve and cuckoo search algorithm that have been recently applied for the computation of SEIG performance parameters in [19], [20], [31], [32], respectively. The four algorithms were executed on the same computer having (Intel (R) Core (TM) i3 CPU@2.53GHz 3,00Go RAM) to minimize the admittance for the following external parameters: load impedance  $Z_1 = 1pu$ , power factor =0.8 lagging, Excitation capacitance  $C=45\mu F$  and rotor speed  $v=1.1 pu$ .

Table 4. Comparison of Taguchi with direct, fsolve, and CS

Algorithm	Solution		Accuracy	Running time in seconds	Tuned parameters
	$X_m$ , pu	F, pu	$ Y $ , $\Omega^{-1}$		
Taguchi	1.7714	0.9624	4.4409e-016	0.1250	1 ( $q$ )
Fsolve [19], [20]	1.7714	0.9624	2.6695e-012	0.1720	-
direct [31]	1.7714	0.9624	1.6063e-009	0.4990	1 ( $\varepsilon$ )
CS [32]	1.7714	0.9624	1.7491e-014	0.1710	3 ( $P_a$ , $\beta$ , $\alpha$ )

As the number of experiments set by the OA used in Taguchi algorithm is 9, the population size in CS algorithm is set to 9 host nests. As for the other algorithms, direct needs the knowledge of search space and fsolve MATLAB built-in function needs only an initial guess. The four algorithms converged to the same solution but with different accuracies and Taguchi algorithm's accuracy is the best one. From the same table, one can notice that Taguchi algorithm requires less time for convergence. It has only one parameter being the number of levels that needs a prior tuning. Furthermore, most of the applications assign a number of two or three to this parameter. In other words, it is not a random number while direct's accuracy is very sensitive to the value of  $\varepsilon$  that is randomly tuned. Cuckoo search algorithm needs three parameters to be tuned and its convergence depends on the appropriate selection of these parameters. As for fsolve MATLAB function, it has no parameter to be tuned but needs an accurate initial guess for convergence. In addition to the accuracy, convergence time and required tuned parameters, Taguchi algorithm is based on simple instructions and arithmetic operations which make it the simplest for implementation.

## 7. EXPERIMENTAL VALIDATION

In order to evaluate the performance of the Taguchi algorithm in the analysis of the SEIG steady state performance, computed results are compared to the experimental one quoted from [18]. Figure 12 illustrates the schematic diagram of the experimental setup where the SEIG is driven by a prime mover. A dc motor is employed to emulate the wind turbine and spin the induction generator's rotor with variable speed. A variable three-phase capacitor bank is connected at the output of the three-phase stator terminals to provide the machine with the required excitation or reactive power. The generator's terminal voltage is connected to a variable three-phase load. The latter can be resistive, inductive or capacitive load.

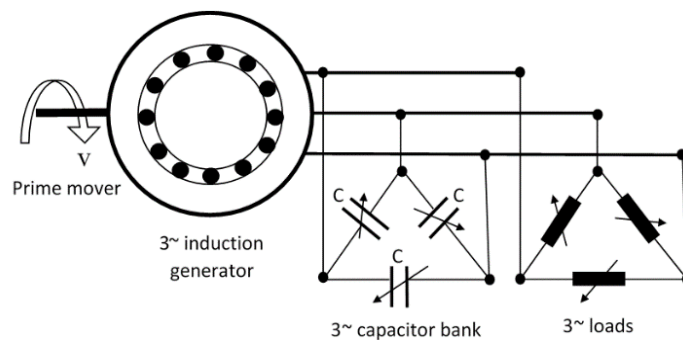


Figure 12. Schematic diagram of three-phase self-excited induction generator

The per-phase equivalent circuit parameters and the ratings of the squirrel cage asynchronous machine are provided in (10). The experimental magnetization characteristic of this machine and its fitted curve which illustrates the change of the air-gap voltage versus the magnetizing reactance, is given in Figure 13. This curve is obtained by performing the open circuit test with different values of the stator voltage while neither the excitation capacitor nor the load are connected to the stator terminals. This test consists in driving the induction generator with constant speed (that is the synchronous speed) and applying a variable three-phase voltage across the stator terminals then measure the stator current. The operation of the rotor at synchronous speed ( $F=v$ ) allows to make the current in the rotor equals to zero as shown in Figure 1. A relationship between  $(V/F)$  versus the magnetizing reactance can be found by considering the fact that  $X_M$  is very high compared to the stator leakage reactance and neglecting the iron loss resistance then solving the obtained KVL equation for  $X_M$ . The obtained experimental points (in red color) are shown in Figure 13. Figure 14 shows the measured and the predicted terminal voltage versus the load current variation for the prime mover speeds of  $v=1.167$  pu and  $v=1$  pu while the excitation capacitance in the capacitor bank has been

set to 20μF. The squares on the graph represent the measured results, however, the computed results are provided by changing the impedance value from 1pu to 40pu and are represented in the graph by a continuous line, the optimizer algorithm used for minimizing the admittance provides the values of magnetizing reactance and frequency. The values of the output load voltage and current are predicted by using the provided values (hereafter, magnetizing reactance and frequency) and the fitted magnetization curve.

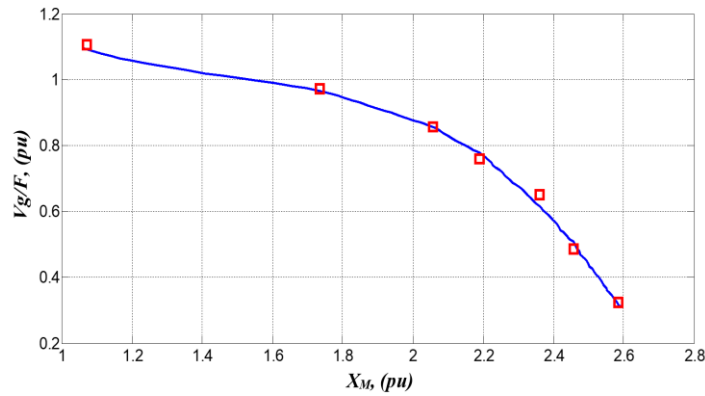


Figure 13. Machine's magnetization curve

It is worth noting that a good agreement between the measured values of load voltage and currents and their predicted ones using Taguchi optimization algorithm. Increasing the load current is achieved by a decrease of the load impedance but this will result in greater terminal voltage drop, Figure 14. Furthermore, according to Figure 7, down to some threshold (minimum load impedance), the machine will be unstable, on the other hand; increasing the excitation capacitance allows the machine to handle higher load current operation but this may exceed its thermal limits. Figure 15 shows the computed and the experimental output voltage of the SEIG unloaded versus the variation of prime mover speed and excitation capacitance of 20μF.

Figure 4 depicting the variation of  $X_M$  versus  $Z_L$  for various values of rotor speed can be used to explain the output voltage variation as a function of rotor speed. That is, for a given load impedance, increasing the rotor speed results in falling of  $X_M$ . The magnetizing curve of the asynchronous generator (Figure 13) shows that  $V_g/F$  gets higher if  $X_M$  decreases even though frequency (F) increases. This means that that increase of  $V_g$  is dominant. In other words, by combining (11) and (12), one can derive the following equation.

$$\overline{V}_L = \overline{V}_g \cdot \frac{(\overline{Y}_A + \overline{Y}_r)}{(\overline{Y}_L + \overline{Y}_C)}$$

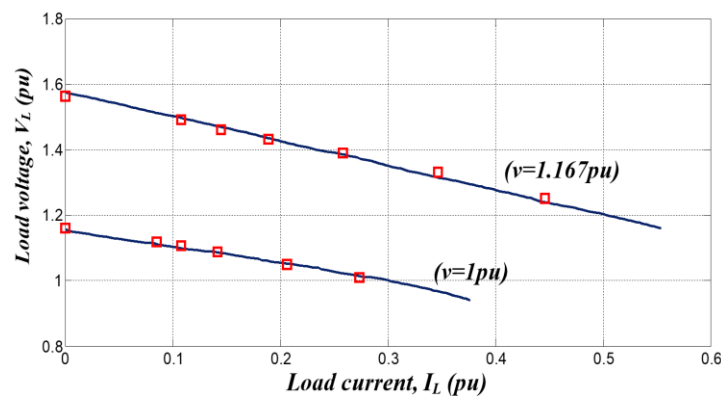


Figure 14. Output voltage with respect to load current for C=20μF and different values of v (v=1 and v=1.167) (continuous line) computed, (squares) experimental

As iron loss is neglected (see Table 5) then  $Y_A$  can be simply substituted by  $Y_M$ . Furthermore,  $Y_r$ ,  $Y_L$ , and  $Y_C$  are constant, while  $Y_M$  and  $V_g$  have increased leading to an increase of  $V_L$ . This explains the good agreement between the predicted voltage across the generator and the measured one. Additionally, for a given prime mover speed, increasing the load current will increase both the magnetizing reactance (see Figure 4) and the load admittance. In addition to that, according to the previous equation, the load voltage across the SEIG will decrease.

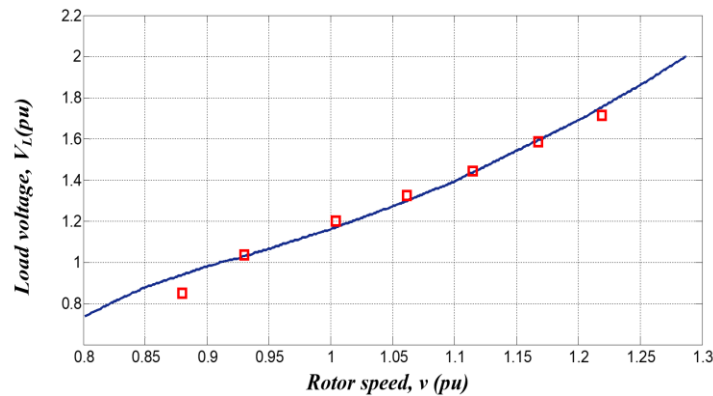


Figure 15. Output voltage versus to rotor speed with motor unloaded and  $C=20\mu\text{F}$ : (continuous line) computed and (squares) experimental

Table 5. Squirrel cage induction machine parameters

Designation	Values
Rated power	750 W
Rated and base voltage, $V_b$	220 V
Rated and base phase current, $I_b$	2.31 A
Rated frequency, $F_b$	60 Hz
Rated speed, N	1800 rpm
Base impedance, $Z_b$	95.24 $\Omega$
Stator resistance, $R_s$	0.1108 pu
Rotor resistance, $R_r$	0.132 pu
Stator reactance, $X_s$	0.1573 pu
Rotor reactance, $X_r$	0.1573 pu
Iron loss resistance, $R_M$ (neglected effect)	$\infty$
Unsaturated value of magnetizing reactance, $X_0$	2.64 pu

## 8. CONCLUSION

In the present paper, a global optimization algorithm based on Taguchi's method is applied to compute the SEIG performance parameters through finding the solution of the admittance equation. The solution is highly sensitive to the input parameters of the SEIG in a way that their variations need an appropriate choice of the initial guess for local search optimization algorithms or an adequate limitation of search space for global optimizers. This difficulty makes various optimization algorithms yielding suboptimal solutions. This difficulty is eliminated by the proposed Taguchi method-based optimization algorithm which is a powerful and an efficient algorithm that can solve the SEIG analysis problem with a high accuracy besides its ease of implementation. The proposed optimization algorithm eliminates: i) The need to first carry out the tedious task of the admittance segregation into real and imaginary parts and the gradient matrix evaluation; ii) The need for the initial guess to start iterations; and iii) The need for an a priori knowledge of the problem for limiting the search space. Results of comparison in terms of accuracy, convergence time and required number of tuned parameters, allows concluding that Taguchi method can be a powerful tool for the evaluation of induction generators performances.

## REFERENCES




- [1] N. A. Qarabash, S. S. Sabry, and H. A. Qarabash, "Smart grid in the context of industry 4.0: an overview of communications technologies and challenges," *Indonesian Journal of Electrical Engineering and Computer Science*, vol. 18, no. 2, pp. 656–665, May 2020, doi: 10.11591/ijeecs.v18.i2.pp656-665.

- [2] N. F. Aswan, M. N. Abdullah, and A. H. Abu Bakar, "A review of combined economic emission dispatch for optimal power dispatch with renewable energy," *Indonesian Journal of Electrical Engineering and Computer Science*, vol. 16, no. 1, pp. 33–40, Oct. 2019, doi: 10.11591/ijeecs.v16.i1.pp33-40.
- [3] R. Choudhary and R. K. Saket, "A critical review on the self-excitation process and steady state analysis of an SEIG driven by wind turbine," *Renewable and Sustainable Energy Reviews*, vol. 47, pp. 344–353, Jul. 2015, doi: 10.1016/j.rser.2015.03.043.
- [4] A. Cheriet *et al.*, "Novel strategy for fault e-diagnosis of wind energy conversion systems using wavelet analysis based on Rt-Lab and Arduino," *International Journal of Power Electronics and Drive Systems (IJPEDS)*, vol. 14, no. 2, pp. 1085–1097, Jun. 2023, doi: 10.11591/ijped.v14.i2.pp1085-1097.
- [5] Y. Majdoub, A. Abbou, and M. Akherraz, "High-performance MPPT control of DFIG with optimized flux reference in presence of nonlinear magnetic characteristic," *International Journal of Power Electronics and Drive Systems (IJPEDS)*, vol. 13, no. 2, pp. 1195–1208, Jun. 2022, doi: 10.11591/ijped.v13.i2.pp1195-1208.
- [6] M. Mokhtari, S. Zouggar, N. K. M'Sirdi, and M. L. Elhafyani, "Voltage regulation of an asynchronous wind turbine using STATCOM and a control strategy based on a combination of single input fuzzy logic regulator and sliding mode controllers," *International Journal of Power Electronics and Drive Systems (IJPEDS)*, vol. 11, no. 3, pp. 1557–1569, Sep. 2020, doi: 10.11591/ijped.v11.i3.pp1557-1569.
- [7] A. J. Ali, M. Y. Suliman, L. A. Khalaf, and N. S. Sultan, "Performance investigation of stand-alone induction generator based on STATCOM for wind power application," *International Journal of Electrical and Computer Engineering (IJECE)*, vol. 10, no. 6, pp. 5570–5578, Dec. 2020, doi: 10.11591/ijece.v10i6.pp5570-5578.
- [8] M. T. Alkhayat, Z. S. Mohammed, and A. J. Ali, "Performance improvement of stand-alone induction generator using distribution SSC for wind power application," *Bulletin of Electrical Engineering and Informatics*, vol. 11, no. 2, pp. 589–601, Apr. 2022, doi: 10.11591/eei.v11i2.2730.
- [9] G. K. Singh, "Self-excited induction generator research—a survey," *Electric Power Systems Research*, vol. 69, no. 2–3, pp. 107–114, May 2004, doi: 10.1016/j.epr.2003.08.004.
- [10] R. C. Bansal, "Three-phase self-excited induction generators: an overview," *IEEE Transactions on Energy Conversion*, vol. 20, no. 2, pp. 292–299, Jun. 2005, doi: 10.1109/TEC.2004.842395.
- [11] S. P. Singh, B. Singh, and M. P. Jain, "Performance characteristics and optimum utilization of a cage machine as capacitance excited induction generator," *IEEE Transactions on Energy Conversion*, vol. 5, no. 4, pp. 679–685, 1990, doi: 10.1109/60.63139.
- [12] S. S. Murthy, B. P. Singh, C. Nagamani, and K. V. V. Satyanarayana, "Studies on the use of conventional induction motors as self-excited induction generators," *IEEE Transactions on Energy Conversion*, vol. 3, no. 4, pp. 842–848, 1988, doi: 10.1109/60.9360.
- [13] S. P. Singh, B. Singh, and M. P. Jain, "Comparative study on the performance of a commercially designed induction generator with induction motors operating as self excited induction generators," *IEE Proceedings C Generation, Transmission and Distribution*, vol. 140, no. 5, pp. 374–380, 1993, doi: 10.1049/ip-c.1993.0055.
- [14] A. K. Al Jabri and A. I. Alolah, "Limits on the performance of the three-phase self-excited induction generators," *IEEE Transactions on Energy Conversion*, vol. 5, no. 2, pp. 350–356, Jun. 1990, doi: 10.1109/60.107232.
- [15] E. Muljadi, C. P. Butterfield, H. Romanowitz, and R. Yinger, "Self-excitation and harmonics in wind power generation," *Journal of Solar Energy Engineering*, vol. 127, no. 4, pp. 581–587, Nov. 2005, doi: 10.1115/1.2047590.
- [16] L. Ouazene and G. McPherson, "Analysis of the isolated induction generator," *IEEE Transactions on Power Apparatus and Systems*, vol. PAS-102, no. 8, pp. 2793–2798, Aug. 1983, doi: 10.1109/TPAS.1983.317962.
- [17] T. F. Chan, "Analysis of self-excited induction generators using an iterative method," *IEEE Transactions on Energy Conversion*, vol. 10, no. 3, pp. 502–507, 1995, doi: 10.1109/60.464874.
- [18] A. L. Alolah and M. A. Alkanhal, "Optimization-based steady state analysis of three phase self-excited induction generator," *IEEE Transactions on Energy Conversion*, vol. 15, no. 1, pp. 61–65, Mar. 2000, doi: 10.1109/60.849117.
- [19] M. H. Haque, "A novel method of evaluating performance characteristics of a self-excited induction generator," *IEEE Transactions on Energy Conversion*, vol. 24, no. 2, pp. 358–365, Jun. 2009, doi: 10.1109/TEC.2009.2016124.
- [20] M. H. Haque, "Comparison of steady state characteristics of shunt, short-shunt and long-shunt induction generators," *Electric Power Systems Research*, vol. 79, no. 10, pp. 1446–1453, Oct. 2009, doi: 10.1016/j.epr.2009.04.017.
- [21] K. A. Nigim, M. M. A. Salama, and M. Kazerani, "Identifying machine parameters influencing the operation of the self-excited induction generator," *Electric Power Systems Research*, vol. 69, no. 2–3, pp. 123–128, May 2004, doi: 10.1016/j.epr.2003.08.003.
- [22] T. F. Chan and L. L. Lai, "Capacitance requirements of a three-phase induction generator self-excited with a single capacitance and supplying a single-phase load," *IEEE Transactions on Energy Conversion*, vol. 17, no. 1, pp. 90–94, Mar. 2002, doi: 10.1109/60.986443.
- [23] A. I. Alolah and M. A. Alkanhal, "Analysis of three phase self-excited induction generator under static and dynamic loads," in *2007 IEEE International Electric Machines & Drives Conference*, May 2007, pp. 1783–1786, doi: 10.1109/IEMDC.2007.383700.
- [24] D. Joshi, K. S. Sandhu, and M. K. Soni, "Performance analysis of three-phase self-excited induction generator using genetic algorithm," *Electric Power Components and Systems*, vol. 34, no. 4, pp. 461–470, Apr. 2006, doi: 10.1080/15325000500346800.
- [25] S. Velusami and S. Singaravelu, "Steady state modeling and fuzzy logic based analysis of wind driven single phase induction generators," *Renewable Energy*, vol. 32, no. 14, pp. 2386–2406, Nov. 2007, doi: 10.1016/j.renene.2006.09.002.
- [26] G. K. Singh, A. S. Kumar, and R. P. Saini, "Selection of capacitance for self-excited six-phase induction generator for stand-alone renewable energy generation," *Energy*, vol. 35, no. 8, pp. 3273–3283, Aug. 2010, doi: 10.1016/j.energy.2010.04.012.
- [27] G. K. Singh, A. S. Kumar, and R. P. Saini, "Performance analysis of a simple shunt and series compensated six-phase self-excited induction generator for stand-alone renewable energy generation," *Energy Conversion and Management*, vol. 52, no. 3, pp. 1688–1699, Mar. 2011, doi: 10.1016/j.enconman.2010.10.032.
- [28] B. A. Nasir, "An accurate dynamical model of induction generator utilized in wind energy systems," *Indonesian Journal of Electrical Engineering and Computer Science*, vol. 27, no. 3, pp. 1185–1198, Sep. 2022, doi: 10.11591/ijeecs.v27.i3.pp1185-1198.
- [29] H. H. Kadhum, A. S. Alkhafaji, and H. H. E. H. Emawi, "The influence of iron losses on selecting the minimum excitation capacitance for self-excited induction generator (SEIG) with wind turbine," *Indonesian Journal of Electrical Engineering and Computer Science*, vol. 19, no. 1, pp. 11–22, Jul. 2020, doi: 10.11591/ijeecs.v19.i1.pp11-22.
- [30] A. Dalabeeh, A.-M. Anwar, T. M. Younes, A. Al-Rawashdeh, and A. Hindi, "Increasing the required slip range of wound induction generator in wind power systems," *Bulletin of Electrical Engineering and Informatics*, vol. 9, no. 2, pp. 436–442, Apr. 2020, doi: 10.11591/eei.v9i2.1795.




- [31] A. Kheldoun, L. Refoufi, and D. E. Khodja, "Analysis of the self-excited induction generator steady state performance using a new efficient algorithm," *Electric Power Systems Research*, vol. 86, pp. 61–67, May 2012, doi: 10.1016/j.epsr.2011.12.003.
- [32] H. M. Hasanien and G. M. Hashem, "A cuckoo search algorithm optimizer for steady-state analysis of self-excited induction generator," *Ain Shams Engineering Journal*, vol. 9, no. 4, pp. 2549–2555, Dec. 2018, doi: 10.1016/j.asej.2017.07.003.
- [33] W.-C. Weng, F. Yang, and A. Elsherbeni, "Electromagnetics and antenna optimization using Taguchi's method," in *Synthesis Lectures on Computational Electromagnetics (SLCE)*, 2008.
- [34] Y. Kuo, T. Yang, and G.-W. Huang, "The use of a grey-based Taguchi method for optimizing multi-response simulation problems," *Engineering Optimization*, vol. 40, no. 6, pp. 517–528, Jun. 2008, doi: 10.1080/03052150701857645.
- [35] K. Aissa, R. Larbi, and K. D. Eddine, "Application of new optimisation algorithm to self-excited induction generator analysis," in *4th International Conference on Power Engineering, Energy and Electrical Drives*, May 2013, pp. 409–414. doi: 10.1109/PowerEng.2013.6635642.

## BIOGRAPHIES OF AUTHORS






**Rachid Boukenoui**    received a master degree in electrical engineering from Blida 1 University, Algeria, Ph.D. degree in electrical engineering from the same university, in 2017. He used to hold several administrative posts with the renewable energies department, Blida 1 University, from 2017 up till day, including the deputy head of department, member of the scientific council and renewable energies license training manager. He has supervised and co-supervised more than 15 masters' students, He has authored or coauthored many publications: with more than 460 citations. His current research interests include: photovoltaic systems, energy conversion, and power electronics. his current project is 'application of new algorithms (AI and metaheuristic) to enhance power harvesting in renewable energy systems'. He can be contacted at email: boukenoui\_rachid@univ-blida.dz or rachidboukenoui@gmail.com.



**Rafik Bradai**    graduated as an engineer in 1997 from the former National Institute of Hydrocarbon and Chemistry. He received a magister and doctorate degrees both in electrical engineering from Boumerdes University (UMBB) in 2001 and 2007, respectively. He was assistant professor at Blida 1 University since 2008. From 2012 to 2014, He was the Head of Electronics Department, Blida 1 University, in Algeria. He used to hold several posts such as: member of the scientific council the university. His fields of interest are control of electrical drives and renewable energies. He can be contacted at email: r.bradai@gmail.com.



**Aissa Kheldoun**    graduated as an engineer in electromechanics from the National Institute of Hydrocarbon and Chemistry, in 1997. He went on to receive his magister, doctorate, and habilitation degrees in electrical engineering from Boumerdes University in 2001, 2007, and 2012, respectively. He joined the IGEE in 2003, where he currently holds the position of professor. His research areas include power electric drives, electronics, energy conversion systems, AI, and metaheuristic algorithms. He has published a book and over 60 journal and conference papers in his fields of interest. He can be contacted at email: aissa.kheldoun@univ-boumerdes.dz or aissakheldoun@gmail.com.